AIP ADVANCES 7, 035212 (2017)

Effect of interface roughness on Auger recombination in semiconductor quantum wells

Chee-Keong Tan,[1,2,a] Wei Sun,[1] Jonathan J. Wierer, Jr.,[1] and Nelson Tansu[1,b]
[1]*Center for Photonics and Nanoelectronics, Department of Electrical and Computer Engineering, Lehigh University, Bethlehem, Pennsylvania 18015, USA*
[2]*Department of Electrical and Computer Engineering, Clarkson University, Potsdam, New York 13699, USA*

(Received 30 November 2016; accepted 5 March 2017; published online 13 March 2017)

Auger recombination in a semiconductor is a three-carrier process, wherein the energy from the recombination of an electron and hole pair promotes a third carrier to a higher energy state. In semiconductor quantum wells with increased carrier densities, the Auger recombination becomes an appreciable fraction of the total recombination rate and degrades luminescence efficiency. Gaining insight into the variables that influence Auger recombination in semiconductor quantum wells could lead to further advances in optoelectronic and electronic devices. Here we demonstrate the important role that interface roughness has on Auger recombination within quantum wells. Our computational studies find that as the ratio of interface roughness to quantum well thickness is increased, Auger recombination is significantly enhanced. Specifically, when considering a realistic interface roughness for an InGaN quantum well, the enhancement in Auger recombination rate over a quantum well with perfect heterointerfaces can be approximately four orders of magnitude. © *2017 Author(s). All article content, except where otherwise noted, is licensed under a Creative Commons Attribution (CC BY) license (http://creativecommons.org/licenses/by/4.0/).* [http://dx.doi.org/10.1063/1.4978777]

I. INTRODUCTION

Auger recombination is a fundamental nonradiative recombination process that exists in all semiconductors,[1] and is theoretically determined by using the appropriate band structure and quantum states in Fermi's Golden Rule. In homogeneous, or "bulk", semiconductors Auger recombination is limited, because of conservation of energy and momentum. However, when a lower bandgap semiconductor is restricted in space by higher bandgap semiconductors (or barriers) to form quantum states, Auger recombination rates can become appreciable. The most widely used and technologically important restriction method for semiconductors is the quantum well (QW), where quantum states are formed and the density of states is reduced via layering of different bandgap semiconductors. QWs not only increase favorable carrier recombination processes such as spontaneous emission and optical gain over bulk semiconductors, but also affects Auger recombination. Understanding Auger recombination in QWs is important, particularly for QW-based optical devices, because at high carrier densities it can become the dominant (and detrimental) recombination mechanism.

Although Auger recombination has been studied extensively in various technologically important semiconductors,[1–28] the convergence of experimental and theoretical results is lacking. This discrepancy is most notable in III-nitride semiconductor alloys,[13–28] and complicates their advancement in important applications such as solid-state lighting and lasers.[29–38] It is now becoming clearer via experimental results that Auger recombination is present in III-nitrides,[14] and causes a detrimental

[a]Electronic mail: ctan@clarkson.edu
[b]Electronic mail: tansu@lehigh.edu

 © Author(s) 2017

decrease in radiative efficiency of light-emitting diodes (LEDs) operating at high operating current densities.[30] However, this result is non-intuitive because simplified models of Auger recombination rates predict a decrease in Auger recombination rates with increased bandgap, and therefore, Auger recombination should not be a concern in wide bandgap III-nitrides.[13] Complex theoretical studies have confirmed this simplification with calculated Auger recombination rates at much lower values when compared to experimental predictions.[13] Even though the recent work on indirect Auger processes such as phonon and compositional. The disconnect between theoretical and experimental results has created confusion and has hindered progress in III-nitride research.

In theoretical calculations of Auger recombination abrupt heterointerfaces are assumed between the quantum well and barrier layers.[2–13,21,22] However, in practice the roughness of this heterointerface is always present, in spite of advances in epitaxial crystal growth techniques such as molecular beam epitaxy (MBE) and metal organic chemical vapor deposition (MOCVD).[39,40] Specifically, for GaAs QWs with AlGaAs energy barrier layers the interface roughness is one to two monolayers (3-5 Å),[41] for InGaAs/InP QW/barriers it is one to four monolayers,[42] and InGaN/GaN QW/barriers it is one to six monolayers (3-18 Å).[43–45] The variation in the InGaN QW is notable because it is considerably large when compared to the typical quantum well thickness (L_{QW}) that is in the range of 2-3 nm. Clearly, interface roughness is a feature of all semiconductor QWs, and the role of interface roughness has been discussed for the photoluminescence line shape analysis for QW.[46,47] Yet interface roughness is ignored in Auger recombination calculations, and is not discussed qualitatively and quantitatively. One would expect rougher interfaces will affect the quantum states and subsequently the recombination probability between states. However, it is an unknown exactly how interface roughness impacts the Auger recombination process in QWs.

In this article, we present a theoretical analysis of Auger recombination in semiconductor QWs, comparing QWs with varying degrees of interface roughness. The interface roughness is shown to play an important role, causing a large increase in the Auger recombination rate because of the additional energy states that can participate in the process. In the technologically important III-nitride semiconductors the increase can be four orders of magnitude over a QW with perfect heterointerfaces illustrating the importance of including interface roughness when calculating Auger recombination rates.

II. AUGER RECOMBINATION THEORY WITH INTERFACE ROUGHNESS

In the direct Auger recombination process (e.g. CHCC process), as illustrated in Fig. 1a, the energy released from recombination of an electron-hole pair is transferred to a third carrier. As a result, the carrier receiving the released energy is excited to a higher-energy final state[48] that also satisfies conservation of energy and momentum. The Auger recombination rate R_{Auger} can be expressed as:[21]

$$R_{Auger} = 2\frac{2\pi}{\hbar}\left(\frac{A}{8\pi^3}\right)^3 \int\int\int\int \left|M_{1,1',2,2'}\right|^2 P_{1,1',2,2'} \times \delta\left(E_{sum}\right) \times \delta\left(\vec{k}_{sum}\right) d\vec{k}_1 d\vec{k}_{1'} d\vec{k}_2 d\vec{k}_{2'}, \quad (1)$$

where $\hbar$ is the Planck's constant, A is the quantum well area, $M_{1,1',2,2'}$ is the matrix element, and $P_{1,1',2,2'}$ accounts for the occupation probabilities of the carriers. E_{sum} and $\vec{k}_{sum}$ stand for $E_{1'} + E_{2'} - E_1 - E_2$ and $\vec{k}_{1'} + \vec{k}_{2'} - \vec{k}_1 - \vec{k}_2$ (k-selection rule), respectively. In equation (1), state 1 and 2 (represented by subscripts) are for electrons in the lower states of the conduction band, while state 1' is for a heavy hole in the valence band and state 2' is for an excited electron in the higher state of the conduction band. The $\delta(k)$ and $\delta(E)$ correspond to the Dirac-delta function of momentum and energy, respectively.

Our analysis of interface roughness in QWs uses Equation (1), and we begin with describing the interface roughness for a QW with barrier layers of infinite potential energy, in order to gain a qualitative understanding of Auger recombination. Figs. 1b and 1d show the schematic representation of this QW system with and without interface roughness between the QW and barrier layers. The average interface roughness, ΔL, is the fluctuation of the interface around the ideal (flat) interface. This roughness is formed by imperfections caused by intrinsic reasons such as strain between materials and alloy disorder, and extrinsic factors such as flaws in epitaxial growth.[40]

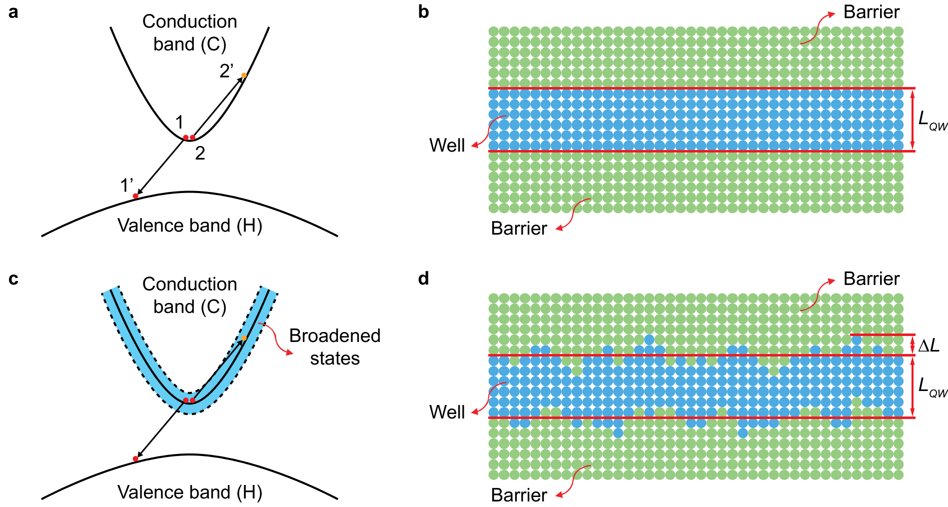

FIG. 1. **Auger process and QW structure. a**, E-k diagram showing a typical band-to-band CHCC Auger recombination process for a QW without interface roughness. **b**, Illustration of a QW without interface roughness sandwiched by two barrier layers, where the L_{QW} represents the thickness of quantum well. **c**, E-k diagram showing the broadened states in the conduction band for the CHCC Auger process of a QW with interface roughness. **d**, Illustration of a QW with interface roughness between the well and the barriers, where the ΔL represents the average interface roughness.

The resulting fluctuations in QW thickness, L_{QW}, will result in fluctuations in the momentum of the confined quantum states. For an ideal QW with infinite barriers the momentum perpendicular to the quantum well, k_z, is inversely proportional to the QW thickness, expressed as:

$$k_z = \frac{\pi}{L_{QW}}. \tag{2}$$

However, since various degrees of interface roughness exist in a realistic QW, the fluctuation of QW thickness (ΔL) directly results in an uncertainty of the perpendicular momentum (Δk_z), resulting in:

$$\frac{\Delta k_z}{\Delta L} = -\frac{\pi}{{L_{QW}}^2}. \tag{3}$$

This perpendicular momentum uncertainty has to be taken into account in the energy dispersion relation of quantum states, expressed as:

$$E = \frac{\hbar^2(k_z \pm \Delta k_z)^2}{2m^*} + \frac{\hbar^2\left({k_{||}}^2\right)}{2m^*}, \tag{4}$$

where m^* is the effective mass, and $k_{||}$ denotes the wave number (or momentum) in the in-plane direction (representing the in-plane momentum). Equation (4) can then be expanded and simplified. Assuming Δk_z is relatively small one can express the energies of the quantum states as:

$$E \cong \frac{\hbar^2 {k_z}^2}{2m^*} + \frac{\hbar^2}{2m^*}\left(k_{||} \pm \frac{k_z \Delta k_z}{k_{||}}\right)^2. \tag{5}$$

Thus, the uncertainty in the QW thickness ultimately leads to an uncertainty in the QWs energy states. This is schematically represented in the E-k diagram in Fig. 1c for the QW with interface roughness. The uncertainty leads to a broader range of available final quantum states for excited carriers, and a higher probability of successive Auger transitions. As a result of this larger amount of available states we expect an increase in the Auger recombination with increased interface roughness.

To incorporate the interface roughness into the calculation of Auger recombination rates, for $a \to 0$, we express the fluctuations and relaxation of the momentum conservation with $\sin(k/a)/\pi k$ (sinc function), replacing the $\delta(k)$ function used for abrupt interfaces in equation (1).[2] In the sinc

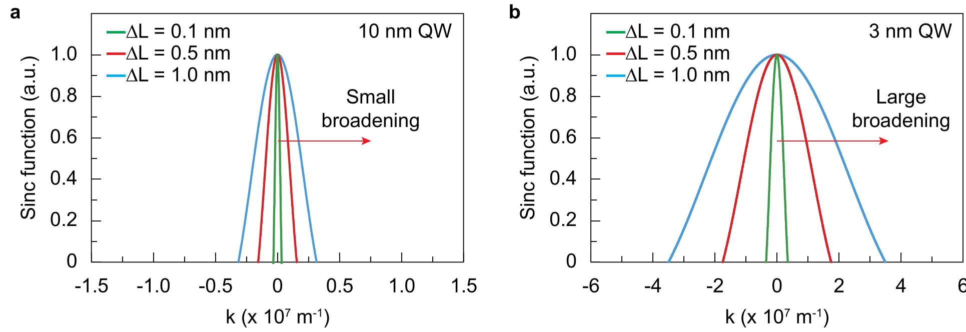

FIG. 2. **The broadening of k-selection in a QW with interface roughness. a**, Increment of interface roughness in a 10 nm QW yields relatively small broadening of the sinc function. **b**, Increment of interface roughness in a 3 nm QW results in larger broadening of the sinc function. The broadening of the k-selection results in larger number of possible Auger transition states, and the comparison of **(a)** and **(b)** shows the effect of interface roughness is more significant in thin QWs compared to thicker QWs.

function the variable, a, is defined as:

$$a = \begin{cases} \frac{2}{L_{QW}}, & \textit{no interface roughness} \\ \frac{\pi}{k_{2'||}} \cdot \frac{\Delta L}{L_{QW}{}^3}, & \textit{with interface roughness} \end{cases}, \tag{6}$$

where the $k_{2'||}$ represents the quasi-momentum for the in-plane wave number in the final state. The variable, a represents a linewidth broadening factor within the sinc function when interface roughness is present, increasing the number of possible Auger transition states attributed to the relaxation of momentum conservation.

Using this formalism, the effect of interface roughness on the Auger transition states with different QW thicknesses is shown in Fig. 2. Fig. 2a and 2b illustrate the lineshapes of the sinc functions for the 3 nm and 10 nm thick QWs as a function of momentum for varying degree of roughness. The linewidth of both QWs resembles a Dirac-delta lineshape when the interface roughness is small (small $\Delta L / L_{QW}$). When the roughness increases, the linewidth of the sinc function also broadens. This linewidth broadening expands the k-selection into a wider range (see Fig. 1c), and increases the allowable Auger transition states in the Auger calculation.

Comparison of Figs. 2a and 2b shows a larger linewidth broadening for the thinner QW (3 nm) compared to the thick QW (10 nm), which is attributed to the larger ratio of interface roughness to QW thickness, $\Delta L / L_{QW}$. This implies that thinner QWs are more sensitive to interface roughness, and we should expect the Auger recombination rate will have larger variation for thinner wells.

For simplicity and to minimize computation time, this study implements a simple parabolic energy dispersion relation for the calculation of Auger recombination rates in the QW. The key message of this computational study is to point to the importance and role of interface roughness on relaxing momentum conservation, which in turn increases the allowable Auger transition states. The implementation of more realistic band structures with large non-parabolicity still needs to be performed in order to provide accurate quantitative comparison of the results.

III. METHODS

Numerical calculations for the Auger recombination process were carried out by using the Monte Carlo approach. Auger recombination rates R_{Auger} are calculated using equation (1) assuming a typical operating carrier density of n = 1 x 10^{19} cm^{-3}. This carrier density is of interest because it is approximately equal to the operating point in LEDs and laser diodes. Then the Auger recombination coefficient C_{Auger} is determined through $C_{Auger} = R_{Auger}/n^3$. In this way our Auger recombination coefficient can be compared to other reports.[15] The band parameters for the III-nitride alloys can be obtained in Ref. 56 and Ref. 57. As an example, the energy band gap of InGaN alloy can be obtained by using the composition-dependent energy band gap equation with bowing parameter set

as 1.4 eV. The calculation of Auger recombination rates is computationally challenging,[9] scaling with the fourth power to the number of k points within the Auger recombination rate equation, and leads to prohibitively expensive computational resources. Therefore, this multidimensional integration is tackled through the use of a Monte Carlo approach. Statistically an average over 40 000 000 Monte Carlo steps are computed in the approach. The numerical calculation procedure to calculate the Auger recombination coefficient is presented in the supplementary material.

IV. AUGER RECOMBINATION RATES IN III-NITRIDE QUANTUM WELLS WITH INTERFACE ROUGHNESS

To demonstrate the effect of interface roughness on Auger recombination rates in QWs we use the III-nitride semiconductor system. The choice of this system, and in particular InGaN QWs, is of interest because they are not only technologically interesting for applications such as high brightness LEDs, but also because strain and epitaxial growth constrains limit QW thicknesses to ~ 3 nm where we believe interface roughness plays an important role. Additionally, QWs formed from InGaN are much thinner than those formed in other semiconductor systems, and have relatively high interface roughness (ΔL ~ 0.6-1.5 nm).[43–45]

The Auger coefficient (C_{Auger}) is plotted as a function of interface roughness (Fig. 3a) and ratio of interface roughness (Fig. 3b) for InGaN QWs with thickness of 3 nm, 10 nm, and 20 nm. For the 3 nm thick QW without interface roughness (ΔL =0) the C_{Auger} is 3.1 x 10^{-34} cm^6s^{-1}, which is in close agreement with previous theoretical results.[13] More importantly, the C_{Auger} for 3 nm thick QW increases abruptly from 3.1 x 10^{-34} cm^6s^{-1} to 1.7 x 10^{-31} cm^6s^{-1} when only 0.1 nm of interface roughness is introduced. Increases hold for thicker QWs too, with increases of C_{Auger} from 1.6 x 10^{-35} cm^6s^{-1} to 1.5 x 10^{-34} cm^6s^{-1} and from 1.3 x 10^{-36} cm^6s^{-1} to 2.8 x 10^{-35} cm^6s^{-1} for 10 nm and 20 nm thick InGaN QWs, respectively. The dramatic increase of C_{Auger} with increased ΔL in the InGaN quantum well is attributed to the increased number of available final states for the excited carrier created by the interface roughness. As the number of available final states increases due to the interface roughness, the probability of an Auger transition is enhanced. Additionally, we find as the ratio of interface roughness to quantum well thickness is increased, Auger recombination is significantly enhanced. At larger interface roughness, from 0.1 nm to 1 nm, the C_{Auger} of all three QWs increases at a slower rate.

These results are interesting because they can explain the discrepancy in theoretical and experimental results for III-nitride QWs. Experimental Auger recombination coefficients are at a much higher value compared to theoretical results that does not consider interface roughness. While including electron-phonon coupling and alloy scattering in Auger recombination calculations[17] can lead to higher theoretical values, we show that including interface roughness can also provide higher values. Including this interface roughness in the calculations is paramount because all realistic III-nitride quantum wells have interface roughness. If we use an interface roughness that is greater than 0.5 nm

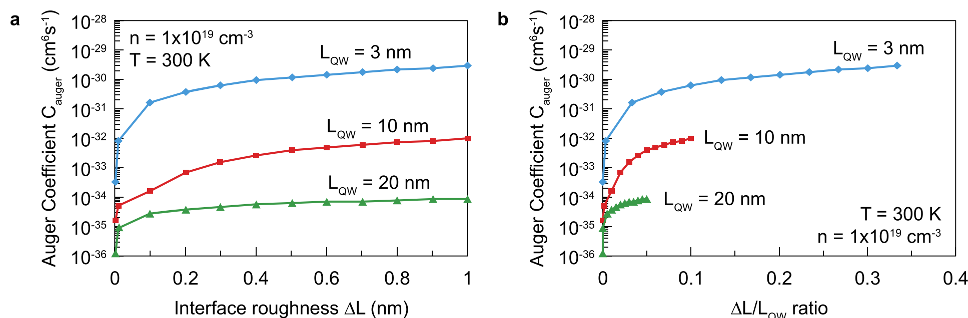

FIG. 3. **The effect of interface roughness. a**, Calculated Auger recombination coefficients in InGaN QWs as function of the interface roughness ΔL with QW thickness of 3 nm, 10 nm, and 20 nm represented by the blue, red and green lines, respectively. **b**, Auger recombination coefficients in InGaN QWs as function of the ratio of interface roughness to QW thickness $\Delta L/L_{QW}$. The QW thickness corresponding to blue, red, and green lines are 3 nm, 10 nm, and 20 nm, respectively.

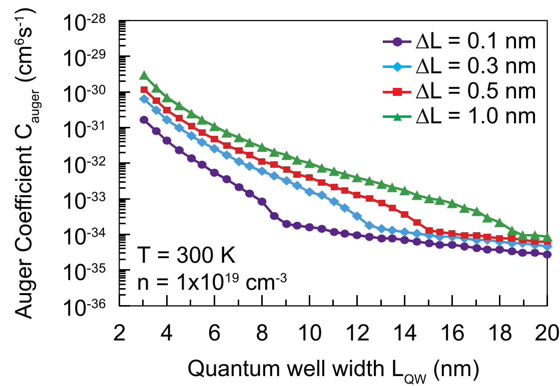

FIG. 4. **The effect of QW thickness on Auger recombination.** Auger recombination coefficients in the InGaN QW are shown as a function of QW thickness from 3 nm to 20 nm with fixed interface roughness. The interface roughness in the case of the purple, blue, red, and green lines equals to 0.1 nm, 0.3 nm, 0.5 nm, and 1 nm, respectively.

than for a typical 3 nm thick QW the Auger coefficient is on the order of 10^{-30} cm^6s^{-1} which is much closer to experimental values.[14]

The value of the C_{Auger} also exhibits a large variation with changing QW thickness. Fig. 4 plots the C_{Auger} of InGaN QW as a function of QW thickness with various fixed interface roughness of 0.1 nm, 0.3 nm, 0.5 nm and 1 nm. The C_{Auger} is reduced by ~ 4 orders of magnitude when the InGaN QW thickness increases from 3 nm to 20 nm for each value of interface roughness (This can also be observed in Fig. 3.). This phenomenon is caused by the weakening of the momentum relaxation when the QW thickness increases, and is separated from the expected reduction in carrier density with thicker wells.[24] This distinction is important because this result suggests that thicker quantum wells will lead to lower Auger recombination rates by *both* lower carrier densities and from a weakening of the momentum relaxation.

Fig. 4 also shows that the C_{Auger} asymptotes to a minimum value with increased QW thickness, and this asymptote value depends on the interface roughness. For example, at an interface roughness of 0.3 nm, the C_{Auger} decreases rapidly from 6.5 x 10^{-31} cm^6s^{-1} to 3.3 x 10^{-34} cm^6s^{-1} when the QW thickness increases from 3 nm to 12 nm, and decreases at a lower rate for thicknesses greater than 12 nm. A similar trend can be observed for all values of interface roughness. Our analysis indicates that increasing the QW thickness (i.e. reducing the $\Delta L/L_{QW}$ ratio) is also important for reducing the Auger rates. However, the effect of suppressing the Auger recombination by using thicker InGaN QW becomes less significant when the QW thickness increases beyond a specific level, thus reducing the role interface roughness plays in controlling and suppressing Auger recombination. Note that if the $\Delta L/L_{QW}$ ratio is small, it is expected that the Auger recombination in the QWs should be approaching that of bulk material systems, similar to the cases reported for the Arsenide-based and Antimonide-based QWs.[11,12]

V. TECHNOLOGICAL IMPLICATIONS

This theoretical study shows the importance of interface roughness in the Auger recombination process of semiconductor QWs. It is important to point out that the current work utilizes only the infinite barrier model for the Auger recombination analysis and further studies will be carried out to provide a more accurate model to understanding interface roughness in QWs with finite barriers. Nonetheless, for InGaN QWs this study is particularly interesting, because the thin QWs and large interface roughness will result in C_{Auger} values that are much higher than what is predicted by using perfect heterointerfaces. For example, assuming a typical InGaN QW thickness of ~ 3 nm, and interface roughness of ~ 0.5 nm the C_{Auger} is ~ 1.2 x 10^{-30} cm^6/s. This value is large enough to cause high Auger recombination rates in visible III-InGaN-based LEDs, and confirms the notion that Auger recombination produces the observed reduced efficiency at high carrier densities (efficiency droop). It is important to note that various mechanisms in addition to Auger recombination process have been

suggested to play a role in the efficiency droop issue.[49–54] However the original cause of efficiency droop is still inconclusive up to this point. On the other hand, our Auger calculations assume direct transitions and do not employ phonons to achieve higher values[17] simplifying the message that Auger recombination is appreciable in III-nitride semiconductors.

These findings also offer an alternative technological solution for controlling and suppressing Auger recombination, and several experimental pathways could be considered. First and foremost, optimizing the material epitaxial growth technique (MOCVD or MBE) could be a useful experimental path to reduce the interface roughness and Auger recombination. Previous studies have demonstrated that the modulation of growth pauses between layers can be used to reduce the interface roughness in the InGaAs QWs,[42] and similar innovations in the growth techniques might also be applied in other semiconductors such as InGaN QWs. Secondly, utilizing thicker QW could suppress the effect of interface roughness on the Auger recombination process, resulting in lower Auger recombination rates. Typically, thicker QWs are desired for lower carrier densities, but the lower Auger recombination rates from a weakening of the momentum relaxation in thicker QWs may also be of benefit too. (Note: For strained and polar materials such as III-nitrides there will be a trade-off with thicker QWs and radiative efficiency because of increased charge separation as the QW becomes thicker.) It is important to point out that the presence of the electric field in the QW will also result in the reduction of electron-hole wavefunction overlap and hence the reduction of Auger recombination coefficients.[18] Finally, developing and implementing surfactant techniques could be important experimental pathway in order to reduce the interface roughness.[55] A combination of the aforementioned methods would potentially minimize interface roughness in semiconductor QWs, and controlling Auger recombination processes for improved device performance.

Our computational study has focused on the essence of the interface roughness on the Auger recombination process in the semiconductor QWs. The model presented in this study implements a simple parabolic energy dispersion relation in order to simplify the Auger recombination calculations. The trend predicted from this finding remains valid within this approximation. In future interface roughness studies, more realistic energy dispersion relationships will be incorporated to more accurately determine the Auger recombination rates in thin (low $\Delta L/L$) semiconductor QWs.

VI. CONCLUSION

In summary, theoretical studies were carried out to evaluate the impact of interface roughness on the Auger recombination process in semiconductor QWs. Our analysis shows that the existence of interface roughness results in a significant enhancement of the Auger recombination process, leading to a large Auger recombination coefficient. The ratio of interface roughness and QW thickness has a strong contribution to the Auger recombination rate in a realistic QW structure with interface roughness. Further analysis shows that the effect of interface roughness on the Auger recombination process is much more significant in a thin QW as compared to a thick QW. Specifically, when considering a InGaN QW with interface roughness, the Auger recombination coefficient is enhanced by two orders of magnitude in the 3 nm thin QW over that in the 20 nm thick QW. In addition, a 3 nm InGaN QW with interface roughness ranging from 0.5 nm to 1 nm, has an $C_{Auger} \sim 10^{-30}$ cm^{6}s^{-1}. This work identifies the importance of interface roughness on the Auger recombination process in the semiconductor QW devices.

SUPPLEMENTARY MATERIAL

See supplementary material for additional discussion of the incorporation of interface roughness in the Auger calculation model for the semiconductor quantum well.

ACKNOWLEDGMENTS

This work was supported by US National Science Foundation (ECCS 1408051 and DMR 1505122), and the Daniel E. '39 and Patricia M. Smith Endowed Chair Professorship Fund.

The author (N.T.) would also like to acknowledge the useful discussion with the late Professor Shun-Lien Chuang (University of Illinois – Urbana Champaign) on the initial concept of this work.

[1] A. R. Beattie and P. T. Landsberg, Proceedings of the Royal Society A **249** (1959).
[2] G. G. Zegrya and A. S. Polkovnikov, Journal of Experimental and Theoretical Physics **86**(4) (1998).
[3] R. I. Taylor, R. A. Abram, M. G. Burt, and C. Smith, Semicond. Sci. Technol. **5**, 90–104 (1990).
[4] C. Smith, R. A. Abram, and M. G. Burt, J. Phys. C: Solid State Phys. **16**, L171–L175 (1983).
[5] N. K. Dutta, J. Appl. Phys. **54**, 1236–1245 (1982).
[6] A. Haug, Semicond. Sci. Technol. **7**, 1337–1340 (1992).
[7] A. Haug, D. Kerkhoff, and W. Lochmann, Phys. Stat. Sol. (b) **89**, 357–365 (1978).
[8] J. Wang, P. V. Allmen, J. P. Leburton, and K. Linden, IEEE J. Quant. Electro. **31**, 864–875 (1995).
[9] D. B. Laks, G. F. Neumark, and S. T. Pantelides, Physical Review B **42**, 5176 (1990).
[10] E. Andreev and A. D. P. O'Reilly, Appl. Phys. Lett. **84**, 1826–1828 (2004).
[11] B. Sermage, D. S. Chemla, D. Sivco, and A. Y. Cho, IEEE Journal of Quantum Electronics **22**, 774–780 (1986).
[12] Y. Jiang, M. C. Teich, and W. I. Wang, Journal of Applied Physics **69**, 836–840 (1991).
[13] J. Hader, J. V. Moloney, B. Pasenow, S. W. Koch, M. Sabathil, N. Linder, and S. Lutgen, Appl. Phys. Lett. **92**, 261103 (2008).
[14] Y. C. Shen, G. O. Mueller, S. Watanabe, N. F. Gardner, A. Munkholm, and M. R. Krames, Appl. Phys. Lett. **91**, 141101 (2007).
[15] K. T. Delaney, P. Rinke, and C. G. Van de Walle, Appl. Phys. Lett. **94**, 191109 (2009).
[16] F. Bertazzi, M. Goano, and E. Bellotti, Appl. Phys. Lett. **97**, 231118 (2010).
[17] E. Kioupakis, P. Rinke, K. T. Delaney, and C. G. Van de Walle, Appl. Phys. Lett. **98**, 161107 (2011).
[18] E. Kioupakis, Q. Yan, and C. G. Van de Walle, Appl. Phys. Lett. **101**, 231107 (2012).
[19] F. Bertazzi, M. Goano, and E. Bellotti, Appl. Phys. Lett. **101**, 011111 (2012).
[20] G. Hatakoshi and S. Nunoue, Appl. Phys. Express **5**, 071001 (2012).
[21] F. Bertazzi, X. Zhou, M. Goano, G. Ghione, and E. Bellotti, Appl. Phys. Lett. **103**, 081106 (2013).
[22] R. Vaxenburg, E. Lifshitz, and AI. L. Efros, Appl. Phys. Lett. **102**, 031120 (2013).
[23] J. Iveland, L. Martinelli, J. Peretti, J. S. Speck, and C. Weisbuch, Phys. Rev. Lett. **110**, 177406 (2013).
[24] N. F. Gardner, Appl. Phys. Lett. **91**, 243506 (2007).
[25] Y.-R. Wu, R. Shivaraman, K.-C. Wang, and J. S. Speck, Appl. Phys. Lett. **101**, 083505 (2012).
[26] A. Laubsch, M. Sabathil, J. Baur, M. Peter, and B. Hahn, IEEE Transactions on electron devices **57**, 79–87 (2010).
[27] A. David and M. J. Grundmann, Appl. Phys. Lett. **96**, 103504 (2010).
[28] A. Laubsch, M. Sabathil, W. Bergbauer, H. Lugauer, M. Peter *et al.*, Phys. Status Solidi C **6**, S913–S916 (2009).
[29] M. H. Crawford, IEEE J. Sel. Top. Quantum Electron. **15**, 1028–1040 (2009).
[30] M. Krames *et al.*, J. Disp. Tech. **3**, 160–175 (2007).
[31] N. Tansu *et al.*, IEEE Photonics Journal **2**, 241–248 (2010).
[32] H. Zhao, G. Y. Liu, J. Zhang, J. D. Poplawsky, V. Dierolf, and N. Tansu, Optics Express **19**, A991–A1007 (2011).
[33] D. F. Feezell, J. S. Speck, S. P. DenBaars, and S. Nakamura, J. Disp. Tech. **9**, 190–198 (2013).
[34] S. P. DenBaars *et al.*, Acta Materialia **61**, 945–951 (2013).
[35] C. K. Tan and N. Tansu, Nature Nanotech. **10**, 107–109 (2015).
[36] X. Li, S. G. Bishop, and J. J. Coleman, Appl. Phys. Lett. **73**, 1179–1181 (1998).
[37] X. H. Li, R. Song, Y. Ee, P. Kumnorkaew, J. F. Gilchrist, and N. Tansu, IEEE Photon. J. **3**, 489–499 (2011).
[38] I. H. Brown *et al.*, IEEE J. Quantum Electron. **42**, 1202–1208 (2006).
[39] N. Nakagawa, H. Y. Hwang, and D. A. Muller, Nature Materials **5**, 204–209 (2006).
[40] J. Singh, *Electronic and Optoelectronic Properties of Semiconductor Structures* Ch. 1, 23–24 (Cambridge University Press, 2003).
[41] H. Sakaki, T. Noda, K. Hirakawa, M. Tanaka, and T. Maysusue, Appl. Phys. Lett. **51**, 1934–1936 (1987).
[42] I. Yamakawa, R. Oga, Y. Fujiwara, Y. Takeda, and A. Nakamura, Appl. Phys. Lett. **84**, 4436–4438 (2004).
[43] G. H. Gu, D. H. Jang, K. B. Nam, and C. G. Park, Microsc. Microanal. **19**, 99–104 (2013).
[44] S. R. Lee, D. D. Koleske, M. H. Crawford, and J. J. Wierer, Jr., J. Crys. Growth **355**, 63–72 (2012).
[45] A. B. Yankovich *et al.*, Microsc. Microanal **20**, 864–868 (2014).
[46] J. Singh and K. K. Bajaj, J. Appl. Phys. **57**, 5433–5437 (1985).
[47] J. Singh, K. K. Bajaj, and S. Chaudhuri, Appl. Phys. Lett. **44**, 805–807 (1984).
[48] L. A. Coldren, S. W. Corzine, and M. L. Masanovic, *Diode Lasers and Photonic Integrated Circuits* Ch. 4, 211–212 (Wiley, 2012).
[49] S. F. Chichibu *et al.*, J. Vac. Sci. Technol. B: Microelectronics and Nanometer Structures **19**, 2177–2183 (2001).
[50] W. W. Chow, M. H. Crawford, J. Y. Tsao, and M. Kneissl, Appl. Phys. Lett. **97**, 121105 (2010).
[51] A. A. Efremov *et al.*, Semiconductors **40**, 605–610 (2006).
[52] M. F. Schubert *et al.*, Appl. Phys. Lett. **91**, 231114 (2007).
[53] X. Guo and E. F. Schubert, J. Appl. Phys. **90**, 4191–4195 (2001).
[54] J. Xie *et al.*, Appl. Phys. Lett. **93**, 121107 (2008).
[55] H. Shimizu, K. Kumada, S. Uchiyama, and A. Kasukawa, Electronics Letters **36**, 1379–1381 (2000).
[56] H. P. Zhao, R. A. Arif, Y. K. Ee, and N. Tansu, IEEE J. Quantum Electron. **45**, 66–78 (2009).
[57] I. Vurgaftman and J. R. Meyer, J. Appl. Phys. **94**, 3675–3696 (2003).

Supplementary Information

Effect of interface roughness on Auger recombination in semiconductor quantum wells

Chee-Keong Tan [1, 2, (a)], Wei Sun [1], Jonathan J. Wierer [1], Jr., and Nelson Tansu [1, (b)]
[1] Center for Photonics and Nanoelectronics, Department of Electrical and Computer Engineering, Lehigh University, Bethlehem, PA 18015, USA
[2] Department of Electrical and Computer Engineering, Clarkson University, Potsdam, NY 13699, USA
(a) Electronic mail: ctan@clarkson.edu
(b) Electronic mail: tansu@lehigh.edu

Calculation Approach – Auger Rate Model with Interface Roughness

1. Average Interface Roughness

Figure S1 schematically represents the interface roughness between the QW and barrier materials. The real interface of the two materials fluctuates around the ideal interface forming imperfections due to intrinsic reasons (e.g. strain between materials, and alloy disorder) and extrinsic factors (e.g. growth technique, and growth condition) [40]. As illustrated in Figure S1, by setting $z = 0$ for the ideal interface, the interface roughness can be characterized by the fluctuations of the well width $\Delta L(\lambda)$ at different lateral position λ. Note that the small imperfections are formed with different sizes at random locations resulting in variations of well width fluctuations at different positions. Therefore, it is difficult to precisely characterize the interface roughness at each position.

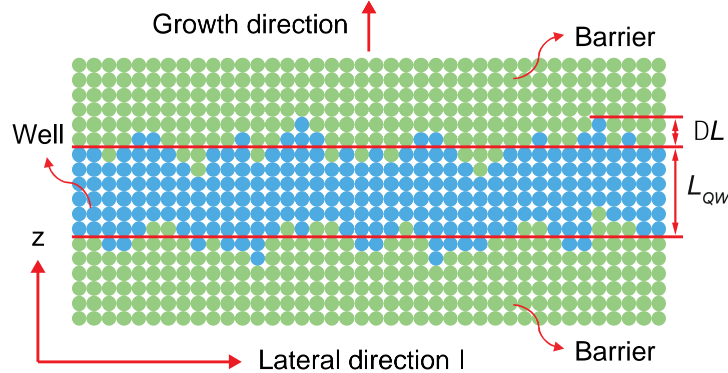

Figure S1: Illustration of the interface roughness at the interface of the well and barrier. The curved line represents the rough interface while the dotted line represents the ideal interface.

In order to address the variations of the interface roughness at different positions, an average interface roughness is used. The average interface roughness can be estimated by taking the root mean square of the interface roughness along the lateral direction. The expression to calculate the average interface roughness ΔL is given as:

$$\Delta L = \sqrt{\frac{1}{\lambda_T}\int_0^{\lambda_T}[\Delta L(\lambda)]^2\, d\lambda} \quad , \tag{1}$$

where λ is the lateral position, λ_T is the length of the active region, and $\Delta L(\lambda)$ is the interface roughness at different lateral position λ. Since the total lateral thickness of a device structure is usually more than a few hundred angstroms [40], the average interface roughness could be effectively smaller than one monolayer depending on the material quality.

2. Uncertainty of In-Plane Momentum

When there are sharp and abrupt interface between the quantum well and the barrier, as the case for an "ideal QW", a simple and ideal energy dispersion relation can be used:

$$E = \frac{\hbar^2({k_z}^2+{k_x}^2+{k_y}^2)}{2m^*} = \frac{\hbar^2({k_z}^2)}{2m^*} + \frac{\hbar^2({k_{||}}^2)}{2m^*} \quad , \tag{2}$$

where ħ is the Planck's constant, m^* is the effective mass, k_z denotes the wave number in the growth direction (representing the perpendicular momentum), and $k_{||}$ denotes the wave number in the in-plane direction (representing the in-plane momentum).

Using an infinite potential well approximation, the perpendicular momentum is inversely proportional to the quantum well thickness,

$$k_z = \frac{\pi}{L_{QW}} \ . \tag{3}$$

However, since various degrees of roughness exist in a "real QW", the fluctuation of well thickness (ΔL) directly results in the perpendicular momentum uncertainty (Δk_z):

$$\frac{\Delta k_z}{\Delta L} = -\frac{\pi}{{L_{QW}}^2} \ . \tag{4}$$

Thus, the perpendicular momentum uncertainty has to be taken into account in the energy dispersion relation

$$E = \frac{\hbar^2(k_z \pm \Delta k_z)^2}{2m^*} + \frac{\hbar^2({k_{||}}^2)}{2m^*} \ . \tag{5}$$

Equation (5) can then be expanded and rewritten into

$$E = \frac{\hbar^2 {k_z}^2}{2m^*} + \frac{\hbar^2}{2m^*}\left({k_{||}}^2 \pm 2k_z\Delta k_z + {\Delta k_z}^2\right) \ , \tag{6}$$

where the perpendicular momentum uncertainty Δk_z is relatively small, so that the square term of Δk_z is negligible in comparison to the two terms of ${k_{||}}^2$ and $2k_z\Delta k_z$. Thus, the ${\Delta k_z}^2$ term can be dropped in equation (6), leading to:

$$E \cong \frac{\hbar^2 {k_z}^2}{2m^*} + \frac{\hbar^2 {k_{||}}^2}{2m^*}\left(1 \pm \frac{2k_z\Delta k_z}{{k_{||}}^2}\right) \ . \tag{7}$$

Note that equation (7) can be approximated to

$$E \cong \frac{\hbar^2 {k_z}^2}{2m^*} + \frac{\hbar^2 {k_{||}}^2}{2m^*}\left(1 \pm \frac{k_z\Delta k_z}{{k_{||}}^2}\right)^2 \ , \tag{8}$$

given that the term $k_z\Delta k_z/{k_{||}}^2$ is sufficiently small. Equation (8) can then be rewritten as:

$$E = \frac{\hbar^2 {k_z}^2}{2m^*} + \frac{\hbar^2}{2m^*}\left(k_{||} \pm \frac{k_z\Delta k_z}{k_{||}}\right)^2 \ . \tag{9}$$

A comparison between equation (2) and equation (9) shows that the fluctuation also results in an in-plane momentum uncertainty ($\Delta k_{||}$), which is specified by:

$$\Delta k_{||} = \pm\frac{k_z\Delta k_z}{k_{||}} \ . \tag{10}$$

By substituting the equation (3) and equation (4) into the equation (10), the expression for the absolute value of the in-plane momentum uncertainty can finally be obtained:

$$\left|\Delta k_{||}\right| = \frac{\pi^2}{k_{||}} . \frac{\Delta L}{{L_{QW}}^3} \ . \tag{11}$$

The resulting in-plane momentum uncertainty from interface roughness as shown in equation (11) implies that the governing momentum conservation condition (Dirac-delta function) in Auger recombination processes is relaxed. It is thus important to take into account the effect of interface roughness in the Auger recombination calculations.

3. Derivation of the parameter *a*

In a quantum well without interface roughness, $\delta(k)$ is replaced with the sinc function of $\sin(k/a)\,/\,\pi k$, where a is $2/L_{QW}$ [2]. In the case of a non-ideal quantum well, the interface roughness has to be taken into consideration in the derivation of a. As the uncertainty of interface roughness results in the

uncertainty of final quantum states, the summation of momentum conservation leads to a net momentum vector $\vec{k}$, which can be described as:

$$\vec{k} = \Delta k_{2'z}\vec{k}_z + \Delta k_{2'||}\vec{k}_{||} \quad . \tag{12}$$

The absolute value of the net momentum vector can then be expressed as:

$$k = \sqrt{(\Delta k_{2'z})^2 + (\Delta k_{2'||})^2} \quad . \tag{13}$$

Using $\Delta k_{||}$ from equation (10), the net momentum vector value can then be described:

$$k = \Delta k_{2'z}\sqrt{1 + \left(\frac{k_{2'z}}{k_{2'||}}\right)^2} \quad . \tag{14}$$

Assuming that the ratio of $k_{2'z}/k_{2'||}$ is much larger than 1, and by replacing $\Delta k_{2'z}$ and $k_{2'z}$ term from equation (3) and (4), the net momentum value can then be expressed as:

$$k = \frac{\pi^2}{L_{QW}{}^3} \cdot \frac{\Delta L}{k_{2'||}} \quad . \tag{15}$$

The root of $\sin(k/a)\,/\pi k$, where k is the variable, yields $na\pi$. Thus, by using equation (15) and taking $n = 1$, the a can then be expressed as:

$$a = \frac{\pi}{L_{QW}{}^3} \cdot \frac{\Delta L}{k_{2'||}} \quad . \tag{16}$$

4. Numerical Formulation of Auger Recombination with Interface Roughness

Figure S2 shows the flow chart of describing the calculation procedure for the Auger recombination coefficient. The momentum values for the carriers in original states are defined, while the energy required for the excitation of a carrier to state 2' as shown in Fig. 1 in the main text is calculated to obtain the corresponding momentum. The calculated momentum is then determined if it satisfies the condition for carrier excitation into state 2', in which the condition takes into account the interface roughness factor as specified in equation (7) in the main text. The satisfaction of the calculated carrier momentum indicates the successful Auger transition, attributed to the carrier excitation into state 2'. By taking into account all the possible Auger transitions, the Auger recombination rates and coefficients can thus be calculated accordingly using the equation (1) in the main text.

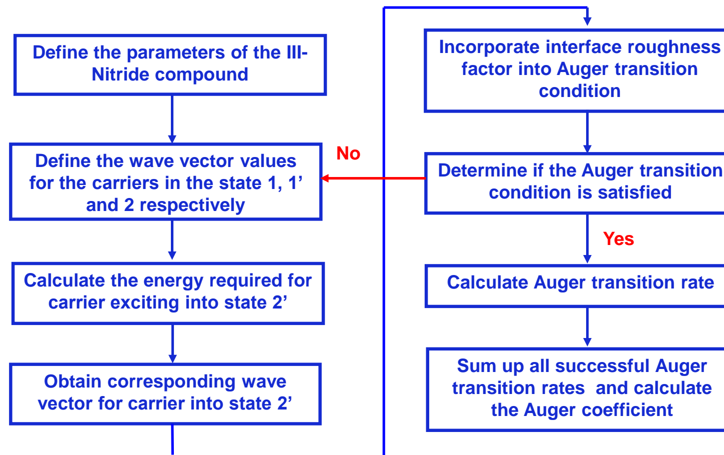

Figure S2: Flowchart of the numerical calculation for the Auger recombination coefficient in III-Nitride QW.